

Advances in Friction-stir Processing of Aluminium Alloys

Daniel N. Wang'ombe, Stephen M. Maranga, Bruno R. Mose and Thomas O. Mbuya

Abstract— Friction-stir processing (FSP) is an inspirational approach to the enhancement of metal properties through grain refinement, homogenization of second phase particles, elimination of defects like porosity, and surface modification among others. Although predominantly applied to aluminium alloys, the reach of FSP has now extended to a variety of materials including steels and polymers. This review deals with the fundamental understanding of the process and its metallurgical consequences. The focus is on microstructure, parameters required for microstructure control and mechanical properties of FSP zone; and FSP of selected aluminium alloys.

Keywords— Friction-stir processing, Friction-stir welding, microstructure modification, grain refinement, recrystallization, surface modification.

I. INTRODUCTION

METHODS for refining grains in metals include inoculation, control of cooling rate during solidification and severe plastic deformation (SPD). However; inoculation and control of cooling rate produce grain of about 150 μm average size. On the other hand; SPD has been used to develop ultrafine grained (UFG) microstructures ((grain size $<1 \mu\text{m}$) in aluminium alloys; resulting in improved mechanical properties, such as, strength, ductility, fatigue strength, fracture toughness and superplasticity [1, 2]. Superplasticity is the ability of a material to sustain tensile elongation $>200\%$ prior to failure. SPD methods include: equal channel angular pressing (ECAP), high pressure torsion (HPT) and Friction stir process (FSP). UFG material with a submicrocrystalline structure can be produced with only a “single pass” of FSP; As compared with ECAP which generally requires several passes [2].

II. FRICTION-STIR PROCESSING

Friction stir processing (FSP) was developed as a generic tool for microstructure modification based on the basic principles of Friction Stir welding (FSW) [3]. Friction stir welding (FSW) was invented in 1991 by Wayne Thomas at The Welding Institute (TWI) in Cambridge, and it has been studied

F D.N. Wang'ombe, Department of Mechanical Engineering, JKUAT (+2540722283492; e-mail: wangombedanielngera@tum.ac.ke).

S.M. Maranga, Department of Mechanical Engineering, JKUAT (e-mail: smmaranga@yahoo.com).

B.R. Mose, Department of Mechanical Engineering, JKUAT (e-mail: mbruno@eng.jkuat.ac.ke).

T.O. Mbuya, Department of Mechanical and Manufacturing Engineering, UoN (e-mail: tmbuya@uonbi.ac.ke).

as a solid state welding technique, especially for aluminium alloys [3,4]

Principles of Friction Stir Welding

Friction-stir welding (FSW) is a solid-state, joining process [5, 6, 7] in which a rotating tool with a shoulder and terminating in a pin, moves along the butting or lapping surfaces of two rigidly clamped plates placed on a backing plate as shown in Fig. 1

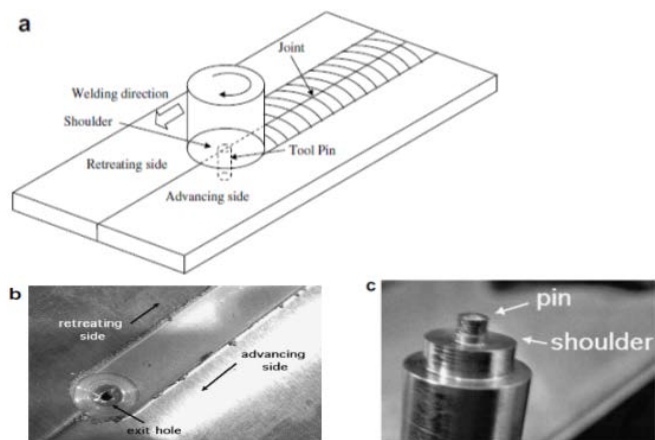


Fig. 1 (a) Schematic illustration of (FSW) process; (b) FSW weld between aluminium sheets; (c) FSW cylindrical tool with a threaded pin [5]

The shoulder makes firm contact with the top surface of the work-piece. Heat generated by friction at the shoulder and to a lesser extent at the pin surface, softens the material being welded. Severe plastic deformation and flow of this plasticised metal occurs as the tool is translated along the welding direction. The material is transported from the front of the tool to the trailing edge where it is forged into a joint.

The half-plate where the direction of rotation is the same as that of welding is called the advancing side, with the other side designated as being the retreating side. This difference can lead to asymmetry in heat transfer, material flow and the properties of the two sides of the weld. For example, the hardness of particular age-hardened aluminium alloys tends to be lower in the heat-affected zone on the retreating side [5]. Once the shoulder makes contact, the adjacent thermally softened region takes up a frustum shape shown schematically in Fig. 2, and corresponds to the overall tool geometry [6]. The region appears much wider at the top surface in contact with the shoulder, tapering down to the pin diameter. A typical cross-section of the FSW joint consists of four zones; namely

base metal (BM), heat-affected zone (HAZ), thermomechanically affected zone (TMAZ), and stirred zone (SZ). The HAZ is similar to that in conventional welds although the maximum peak temperature is significantly less than the solidus temperature, the heat source is rather diffuse, and can lead to somewhat different microstructures when compared with fusion welding processes. The SZ or nugget region containing the “onion-ring” appearance is the one which experiences the most severe deformation, and is a consequence of the way in which the tool deposits material from the front to the back of the weld. The TMAZ lies between the HAZ and SZ; the grains of the original microstructure are retained in this region, but often in a deformed state. FSW results in microstructural changes which influences the weld mechanical properties [7].

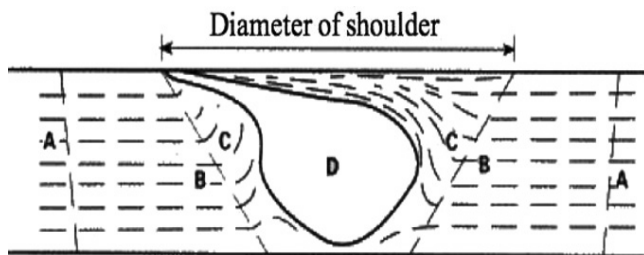


Fig. 2 Schematic cross-section of a typical FSW weld showing four distinct zones: A, B, C and D; namely base metal (BM), heat-affected zone (HAZ), thermomechanically affected zone (TMAZ), and stirred zone (SZ) or nugget or onion zone respectively [5].

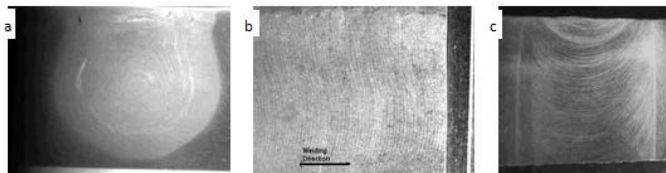


Fig. 3 section views of FSW joint showing the marks at a plane: (a) perpendicular, (b) parallel and (c) traverse to the plane of tool rotation [9].

Various studies have tried to explain the formation of the onion ring in the SZ. The FSW of 2024 to 6061 Al alloys produced intercalated (Swirl and vortex-like) flow patterns in the SZ that were found to be associated with change in tool speed from 400 -1200 rpm [8]. Krishnan [9] found that the 6061 and 7075 FSW joint cross section (a) were characterized by presence of onion rings as shown in Fig. 3. The rings formed swirl patterns in a plane perpendicular to the rotation plane of the tool. Krishnan explained that the formation of onion rings was a geometric effect due to the fact that cylindrical sheets of material were extruded during each rotation of the tool, and cutting through the section of the material produced an apparent ‘Onion Rings’. It was postulated that the tool appeared to wait for a very short time to produce frictional heat and extrude a cylindrical shaped material around to the retreating side of the joint. The spacing of the markings was found to be equal to the forward motion of the tool in one rotation. At a constant feed rate, the spacing

of the rings was found to be inversely proportional to the rotation speed.

A recent study [10] on the role of FSW tool on material flow and weld formation in 7020-T6 alloy, found that there were two different modes of material flow regimes involved in the friction stir weld formation; namely “pin-driven flow” and “shoulder-driven flow”. Material transfer in the pin-driven region took place in successive layers that had crescent cross-section with wide top and narrow bottom, and had an upward flow. The shoulder deflected the pin-driven material from the retreating side to advancing side. The layer thickness in the centre of the weld was comparable with distance travelled per rotation of the tool. These material flow regimes merged, and resulted in formation of a defect-free weld. The etching contrast in the regimes gave rise to onion ring pattern in the FSW joint.

FSW joints are known to be free from defects like porosity, slag inclusion, solidification cracks, etc., and these defects deteriorate the weld quality and joint properties. The defects are minimised due to absence of melting during welding, since the metals are joined in the solid state itself due to the heat generated by the friction and flow of metal by the stirring action. However; FSW joints are prone to other defects like pin holes, tunnel defect, piping defect, kissing bond, cracks, among others. The defects result from improper plastic flow and insufficient consolidation of metal in the FSP region [2]. Defects have been observed when the optimal temperature and hydrostatic pressures are not maintained during FSW [9].

Presently, FSW is commercially used in industries, such as ship-building, high-speed train manufacturing, and aviation industry [30].

The principles of FSP

The concept of FSP technique is similar to that of FSW, and is illustrated in Fig. 4. A high strength tool shown in Fig. 4(c), with a shoulder and a pin attached underneath is used for friction stirring. Heat, generated by the friction between the rotating tool and the material surface and the high-strain-rate plastic deformation, softens the material (without melting). The tool traverses through the material, which is then brought from the front to the back of the tool and forged down under the action of the tool shoulder.

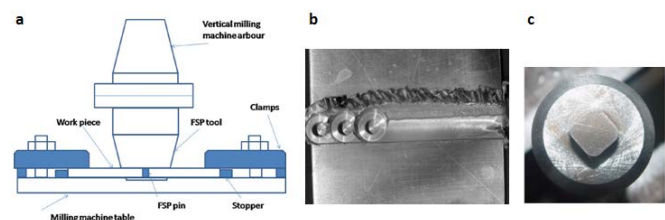


Fig. 4 (a) Experimental set-up of FSP on a milling machine; (b) FSP'ed sample using 3 overlapping passes (c) FSP tool photo showing the tool shoulder and the square pin [11].

Table I Materials and tools used during the FSP/FSW.

Alloy	Material (mm)			Material	Tool specifications (mm)			Ref
	L	W	T		Shoulder (D)	Pin (d/square)	length (L)	
7xxx				Cobalt	11.4	Cylinder (4.2)	4	1
6061	300	150	6	High carbon steel	18 (optimum)	4x4		2
1050	100	22.5	5	hardened SKD 61 (JIS)	7	Conical (3)	3	4
7020	300	75	4.4	(HDS) H13 (tool steel)		Frustum(6,4)	4.2	10
6082	120	100	6	MO-W tool steel	15	Square (6X6)	5	11
7xxx		100	7	Ferro-Titanit	18	8	6.8	15
356			6.35					16
6061	60	20	3.1	HSS (SKH9)	12	3	2.8	16

The tool is normally made of high-speed steel, High carbon steel (the tool steel for hot work) [5], polycrystalline cubic boron nitride, and wolfram alloys as shown in Table I. The tool pin shapes include cylindrical (straight, tapered and threaded), triangular and square. There is evidence that FSP tools have been manufactured from end mills that were ground to size on a circular grinder and it was ensured that they conformed to standard sized collets [14]. Based on data shown in Table I the ratio of tool shoulder (D) to pin diameter (d) is 2.5; and the pin diameter is always equal to the plate thickness. However the length of the pin is slightly less than the plate thickness.

Attempts to modify the structure of materials with the FSP method have been carried out on aluminium, copper, magnesium, steels, and also composites with a metallic matrix [17]. There are six areas of research interest using FSP on rolled or milled aluminium plates. Mainly, FSP has been established as a potential grain refinement technique for Al alloys including 6061 [2], 319 [12], 356 [13], and 6082 [11]. Further; FSP has homogenized second phase particles and minimized porosity [13]. It has been suggested that the FSP technique may be applicable to homogenization of MMC materials with inhomogeneous microstructure [4]. Additionally; local modification of material properties, such as: strength, ductility, hardness, fatigue life, fracture toughness and corrosion resistance have been enhanced [16]. Finally; FSP has been used for the creation of composite structures in the surface layer of the material by the introduction of a strange phase, e.g. carbon nanotubes, SiC, Al₂O₃ and SiO₂ particles, and others [17, 18].

III. MICROSTRUCTURE OF FSP ZONE

If Studies on the microstructure of a friction stir processed (FSP) zone, has demonstrated that it consists of fine recrystallized grains resulting from a severe plastic deformation of the magnitude experienced in equal-channel angular pressing (ECAP) and high-pressure torsion (HPT) [4]. Additionally the recrystallized grain sizes in 1050 [2], 1100, 6061 [8] and 7050 [7] aluminium alloys ranged from 2 to 10 μm . These sizes were approximately 10 to 100 times smaller than in the original work piece materials [4]. FSP was used to create a microstructure with grain size 0.68 μm in as-cast Al-8.9Zn-2.6Mg-0.09Sc (wt.%) alloy [1]. Microstructure of the

FSP zones in 1050 aluminium alloy had recrystallized equiaxed grains of size 0.5- 4 μm [4]. These results suggest that materials with very fine grains, on the scale of microns may be produced through FSP.

The presence of equiaxed and fine grains of 2-10 μm in the SZ of AM60 magnesium alloy was observed. The grain refinement microstructure of the SZ indicated the occurrence of dynamic recrystallization due to concurrent intense plastic deformation and frictional heat. The average grain sizes of the FSP were about 6 μm and 9 μm in the 3,500 rpm and 4,500 rpm friction stir processing trials, respectively.

Grain size measured within the FSP zone ranged between 2.0 and 6.0 μm , depending on the processing parameters [1]. Relatively small second-phase particles in 1050 aluminium alloy were homogeneously distributed in the central region of the FSP zone as compared with the unprocessed zone as shown in Fig 5.

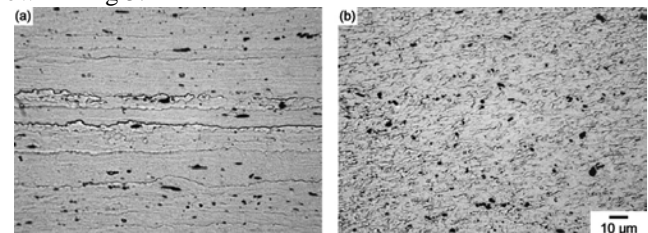


Fig. 5 Comparison of second-phase particles (a) in the unprocessed zone and (b) in the FSP zone of the specimen processed at the tool rotation speed of 560 rpm and the tool traverse speed of 155 mm/min [4].

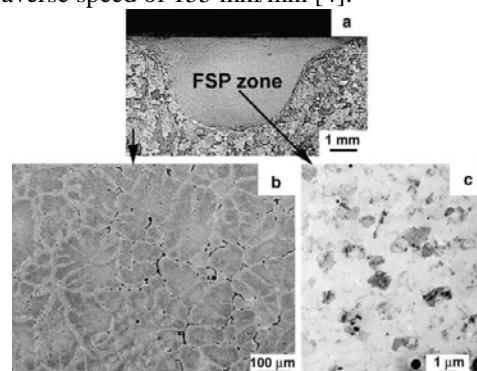


Fig. 6 (a) An optical macrograph of the FSP Al-Zn-Mg-Sc alloy, (b) an optical micrograph of the parent as-cast (unprocessed) material showing typical dendritic microstructure, and (c) a bright field TEM image of the FSP zone, showing ultrafine grains [1].

During the FSP of Al–Zn–Mg–Sc alloy, a combined effect of deformation and temperature lead to very fine grain sizes through the dynamic recrystallization (DRX) process [1,8], as shown in Fig. 6, and break-up of constituent particles [2]. A low peak processing temperature and a fast cooling rate kept the post-DRX growth of grains limited. This, in turn, helped in the generation of the UFG microstructure.

Rolled plates of high strength Al 7050 and Al-Li-Cu alloys have been found to have highly elongated and pancake shaped BM grains [7, 20]. These grains were several hundred micrometers long, approximately 75 μm thick and had average grain diameter of 87 μm . The microstructure of FSW 7050 alloy showed that the BM grains had low angle boundaries, and low dislocation density, and deformation in the TMAZ resulted in severe bending of the grain structure. In contrast, the microstructure within the SZ contained equiaxed grains formed through continuous dynamic recrystallized (CDRX). During CDRX the BM grain low-angle boundaries are replaced by high-angle boundaries in the DXZ by a continuous rotation of the original low-angle boundaries during FSP; under conditions of frictional heating and plastic strain. Consequently; the TMAZ and SZ grains achieves high-misorientation, high dislocation density and high angle grain boundaries. Within the TMAZ, the grain structure of Al 2024 alloy has been reported to be highly elongated and with a considerable grain distortion due to mechanical effect of the tool, and the grain structure of HAZ was observed to be similar that of the BM [21].

Use of a coolant has been found to produce ultrafine grains. Al 6061–T6 plates, with an initial grain size of $\sim 50\mu\text{m}$ were subjected to FSP in air and also under water at speed of 1000 rpm and feed of 1.27 mm/s. The final average grain size for air and submerged process were $\sim 5\mu\text{m}$ and $\sim 200\text{nm}$ respectively [14]. FSP 7075 Al was quenched by pouring methanol and ice on the joint immediately after the withdrawal of the tool [22]. Microstructural characteristics of five samples from the processed material $\sim 0, 0.3, 1$ and 3mm away from the pin, and the fifth sample was prepared from the joint area outside the tool shoulder were investigated. The average grain sizes starting from specimen 1-5 were 0.1-0.4, 0.8, 1.2, 1.5 and 1-4 μm . Initial sizes of newly recrystallized grains of 7050 alloy were 25–100 nm, and grew to 2–5 μm after 1–4 min due to frictional heating at 350–450 $^{\circ}\text{C}$ [23]. Consequently; attempts to minimize the heat generated have prevented the grain growth.

It has been demonstrated that FSP eliminates casting defects like porosity and microsegregation in a single step, and modify the coarser dendritic microstructure into a relatively homogenized one with ultrafine grains (0.68 μm) [1]. The second phase particles have been broken down and distributed homogeneously in the SZ [4]. Within the SZ, and due to the intensified stirring action, the second phase particles were homogeneously dispersed and had almost regular size, whereas, on the TMAZ side the particles size is heterogeneous ranging between coarse to fine particles as shown in Fig. 7. In

addition, the density of particles within the TMAZ has been found to be less than that in the SZ [11]. Therefore, the microstructural development in each region is usually a strong function of the local thermo-mechanical cycle experienced.

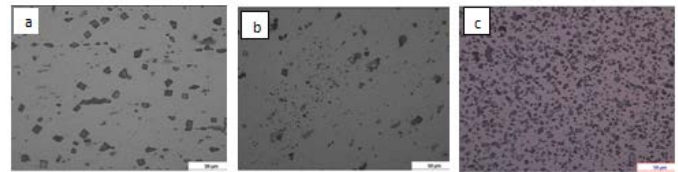


Fig. 7 Second phase particles found in specimen processed at 850 rpm, 90mm/min using one pass taken at different locations: (a) BM, (b) TMAZ and (c) SZ [11].

IV. PARAMETERS REQUIRED FOR MICROSTRUCTURE CONTROL OF THE FSP ZONE

The preparation of UFG Al alloys via FSP has been limited to variation of main parameters including: tool rotational speed, transverse speed (feed rate), the vertical pressure on the tool, the tilt angle of the tool and the tool geometry.

TEM microstructure of the FSP zones in 1050 aluminium alloy at tool rotation speed of 560, 960 and 1840 rpm were composed of recrystallized equiaxed grains 0.5 μm , 1–2 μm and 3–4 μm , respectively [4]. Therefore the recrystallized grain size increased with increase in the maximum temperature from 190 to 310 $^{\circ}\text{C}$, which resulted from the increase in the tool rotation speed. The FSW of 2024 to 6061 Al alloys produced a temperature rise that was directly proportional to increase in tool rotation speeds in the range 400–1200 rpm [8]. Consequently; the grains were observed to grow by 10 to 10^2 times the original recrystallized grain. Further peak temperature has been found to increase significantly with increasing rotational speed and vertical pressure on the tool, and to decrease slightly with transverse speed [4]. Therefore the rise in peak temperature has been found to have a marked increase in the grain size. The feed rate increase has been inversely proportional to grain size [19]; however, it has not shown a significant effect on the grain size [1, 3, 4]. Hence; grain growth is observed with an increase in the processing parameters that promote heat generation.

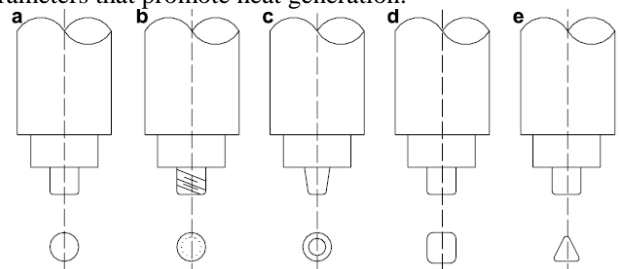


Fig. 8 The five tool pin profiles used in the FSP (a) straight cylindrical (b) tapered cylindrical (c) threaded cylindrical (d) square and (e) triangular [2].

Tool geometry includes the pin diameter (d), pin length (L), pin profile and shoulder diameter (D). Pin profile has been found to play a crucial role in material flow and in turn regulate the transverse speed of the FSP. During the investigation of the Influence of tool pin profile and tool shoulder diameter on the formation of friction stir processing

zone of 6061 and 2219 alloys [2,24], five different tool pin profiles (straight cylindrical, tapered cylindrical, threaded cylindrical, triangular and square) as shown in Fig. 8 were used, and each profile had three different shoulder diameters.

Eccentricity of the pin allows the hydromechanically incompressible plasticised material to flow more easily from the leading edge to the trailing edge of the rotating tool [6]. Off-centre or non-circular pin allows plasticised material to pass around the pin. The square pin had the highest eccentricity with dynamic volume and static volume in the ratio of 1 to 1.56, and produced the highest stirring pulsating action of 4 pulses per revolution of the tool in the flowing material due to flat surfaces. Consequently, the square profile produced the finest equiaxed grained microstructure, highest tensile strength, greatest microhardness, and least defects. Three shoulder diameters (15, 18 and 21mm) of the square pinned tool were considered. The combined effect of higher eccentricity, higher number of pulsating stirring action during metal flow and an optimum tool shoulder diameter may be the reason for superior tensile properties of the joint fabricated using square pin profiled tool with 18 mm shoulder diameter. Increasing the shoulder diameter has been reported to produce an increase in the heat generated during the FSP, and promoting grain growth [19].

During the investigation of the influence of multi-pass friction stir processing on the properties of alloy 6082, it was found that the accumulated heat accompanying multiple passes resulted in increase in the grain size, dissolution of precipitates and fragmentation of second phase particles [11]. The number of passes had bigger effect than that of the processing parameters.

V. MICRO HARDNESS AND TENSILE PROPERTIES

Vickers microhardness measurements have been conducted across the section of FSW and FSP specimens. Hardness profiles across the SZ, TMAZ, HAZ and BM were found to vary. The microhardness profile of 7005 10% composite shown in Fig. 9 had a minimum hardness in the SZ, accompanied by an increase in the TMAZ to a peak, there after another minima was attained in the interface between TMAZ and HAZ, in the HAZ the hardness increased [15]. However; in another study [11] on FSP of alloy 6082, the lowest microhardness was found in the TMAZ on the advancing side and hardness was found to rise in the BM as shown in Fig. 10 (a). The study failed to distinguish the HAZ from the BM. Additionally from the two studies, it is not clear whether the hardness profile in the TMAZ is increasing or decreasing. Unlike in the hardness of 6082 alloy where the lowest hardness was noted on the advancing side, no significant difference in hardness between the advancing and retreating sides were found in the study of alloy 6061 [16]. The microhardness of the 6061 and 6082 alloys was found to be lowest on the retreating side at the transition between the TMAZ and HAZ, and the point was within the limits of shoulder diameter [25]. In the study of FSW 2024-T351 alloy the SZ was found to be significantly harder than the region of TMAZ immediately outside the SZ boundary [21]. The point of minimal hardness

in 5083 alloy has been found [26] to possess high residue stress and tensile fracture occurred at the point in both the 6082 and 6061 alloys [25].

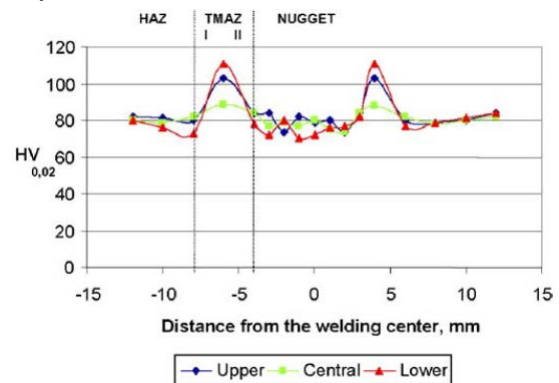


Fig. 9 Hardness profiles on the cross-section of the FSW 7005 10% Al_2O_3 composite [15]

Microhardness measurement results of 6082 and 6061 alloy are as shown in Fig. 10 (a) [11] and Fig 10 (b) [16] respectively. In general, it can be seen that the SZ became much softer than the unaffected BM. The relatively high hardness of the base material was due to heat treatment. Softening of SZ with respect to the BM was due to the decomposition of β'' precipitates, over ageing of the precipitates and fragmentation of second phase particles. In addition, the TMAZ experienced more softening than the SZ due to the dissolution and growth of precipitates.

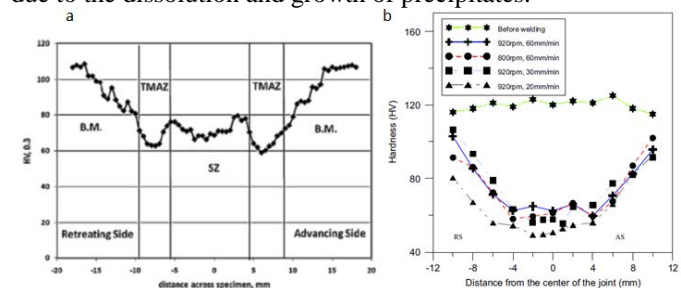


Fig. 10 Hardness distribution across (a) FSP-ed 6082 Al alloy specimen at 850rpm and 140mm/min using two passes [11]; (b) FSW specimen [16].

The microhardness measurements across friction stir welded 2024-T351 joint approximated the lengths of the four distinct zones [21]. The centre of the SZ was significantly harder than the TMAZ immediately outside the SZ, and hardness was lowest in the middle of the TMAZ. There after hardness increased steadily towards the boundary with HAZ, and into the HAZ until the BM hardness was realised. The lengths of the three zones were: the SZ from plate joint line (P JL) extending 5–6 mm out, the TMAZ from 5–6 mm to 10–12 mm, and the HAZ from 10–12 mm to 30–45 mm. The distance from the P JL to the end of the HAZ was approximately 48 mm. The residual hardness of FSW 6061 -T₆ alloy varied from 55 VHN near the top of the weld to 65 VHN near the bottom; in contrast to a workpiece hardness which varied between about 85 and 100 VHN [26]. Microhardness variation across FSW plates of two dissimilar metals shown in Fig. 11b showed a clear distinction between the three zones and the BM [27].

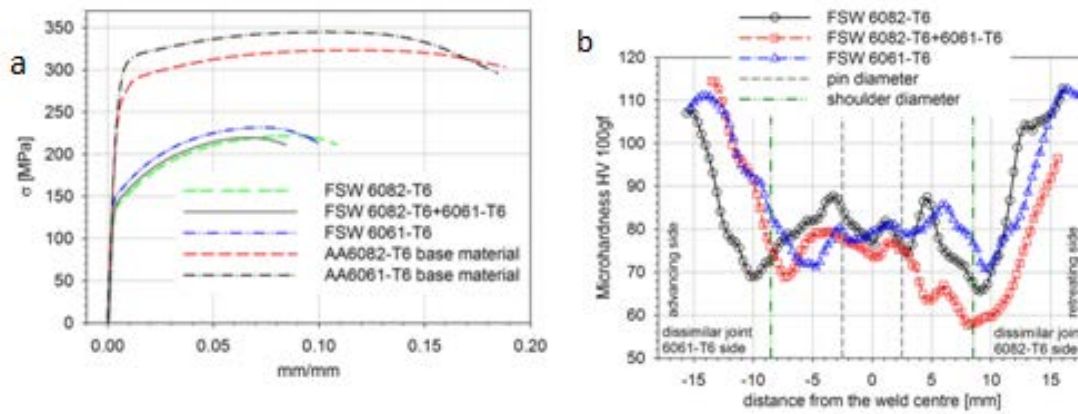


Fig. 11 (a) Tensile tests for FSP specimens and (b) transverse microhardness the specimens [25]

A zone lying in the transition between TMAZ and HAZ on the retreating side had the lowest hardness value [8], and in the case of the mixed joint it was located in the AA6082-T₆ alloy plate side [25].

VI. FSP OF CAST ALUMINIUM SILICON ALLOYS

FSP has been applied to aluminium silicon alloys. Friction stir processing (FSP) was applied to cast 356 Al alloy to modify the as-cast microstructure [13]. FSP eliminated porosity, homogenized and refined the cast microstructure. The resultant microstructure contained fine Si particles (0.25 – 0.42 μm) that were distributed in a fine equiaxed grain aluminium matrix of size 3 – 4 μm . A post-FSP T₆ heat treatment did not alter the Si particle distribution, but did significantly coarsen the Si particles. In another study [12] A319 and A356 castings were treated by friction stir processing to reduce porosity and to create more uniform distributions of second-phase particles. The dendritic microstructures were eliminated in stirred zones. The ultimate tensile strengths, ductility, and fatigue lives of both alloys were increased by the FSP.

VII. FSP OF 6XXX SERIES ALLOYS

The SZ in 6061-T₆ and 6082-T₆ alloy was characterized by a dynamic continuous recrystallization microstructure, and second-phase particles in the workpiece were essentially “stirred” into the weld zone; resulting in a homogeneous structure containing equiaxed grains and a reduced dislocation density [11, 27]. The SZ grain size averaged 10 μm in contrast to 100 μm for the workpiece. Although TMAZ underwent plastic deformation, recrystallization did not fully occur in this zone due to insufficient deformation strain and lower peak temperatures compared to the SZ. As a result it was characterized by a less deformed structure, in which the parent metal-elongated grains were markedly bent due to plastic deformation into the direction inclined to the TMAZ/SZ boundary. The heat affected zone (HAZ) experienced a thermal cycle, without plastic deformation and thus retaining a grain structure similar to the parent material. The residual hardness of this zone varied from 55 VHN near the top of the

weld to 65 VHN near the bottom; in contrast to a workpiece hardness which varied between about 85 and 100 VHN. For the 6061-T₆ and 6082-T₆ alloys it was observed that the minimum microhardness occurred in the transition between TMAZ and HAZ, and on the retreating side [27]. Further tensile failure occurred at the point. An increase of tool rotational speed from 400 to 1200 rpm during the FSW of 2024 to 6061 resulted to rise in temperature to 0.6- 0.8 T_m within the processed zone [8]. Introduction of multi FSP passes on 6082-T₆ alloy was found to raise the temperature too [11]. The heat generated dissolved the β'' precipitates, and upon cooling a softer β' precipitate was formed; hence decrease in hardness. Consequently the microhardness was reduced by about 45%, and the grains were observed to grow by 10 to 10^2 times the original recrystallized grain size [11, 16].

FSP of 6061 aluminum alloy to copper was difficult due to the brittle nature of the intermetallic compounds formed in the SZ [25]. The joining of the dissimilar metals 6061 aluminum alloy and copper weld consisted mainly of several intermetallic compounds such as CuAl_2 , CuAl , and Cu_9Al_4 together with small amounts of $\alpha\text{-Al}$ and the saturated solid solution of Al in Cu. The measured peak temperature in the weld zone of the 6061 aluminum side reaches 580 °C, which was distinctly higher than the melting points of the Al-Cu eutectic.

VIII. CONCLUSION

As the concept of FSP is relatively new, some areas need comprehensive investigation to optimize and make it feasible. On the basis of the literature reviewed it has been observed that there is limited research studies on optimizing the process parameters of friction stir processing of 6000 series alloys. This can reduce heat generation, and hence yield the benefits of improved mechanical properties and arrest grain growth after refinement.

ACKNOWLEDGEMENT

The authors wish to thank the National Research Fund (NRF) and JKUAT Research, Production & Extension (RPE)

Division, for the financial assistance to the ongoing research on the “*Development of Recycle-friendly Aluminum Alloys for Automotive and Structural Applications*” under grant No JKU/2/4/RP/196.

REFERENCES

- [1] Charit I. and Mishra R.S.; (2005); Temperature superplasticity in a friction-stir-processed; *Acta Materialia*, Vol. 53; pp. 4211–4223.
- [2] Elangovan K. and Balasubramanian V.; (2008a); Influences of tool pin profile and tool shoulder diameter on the formation of friction stir processing zone in AA6061 aluminium alloy; *Materials and Design*; Vol. 29; pp. 362–373
- [3] Sen U. and Sharma K.; (2016); Friction Stir Processing of Aluminum Alloys: A Literature Survey; *IJSRSET*; Vol. 2; pp. 771-774
- [4] Kwon Y. J., Saito N. and Shigema I.; (2002); Friction stir process as a new manufacturing technique of ultrafine grained aluminum alloy; *Journal of materials science letters*, Vol. 21; pp. 1473 – 1476
- [5] Nandan R., DebRoy T., and Bhadeshia H.K.D.H.; (2008); Recent advances in friction-stir welding – Process, weldment structure and properties; *Progress in Materials Science*, Vol. 53; pp. 980–1023
- [6] Thomas W. M. and Nicholas E. D.; (1997); Friction stir welding for the transportation industries; *Materials & Design*; Vol. 18; Nos. 4 and 6; pp. 269- 273
- [7] Su J.-Q., Nelson T.W., Mishra R. and Mahoney M.; (2003); Microstructural investigation of friction stir welded 7050- T651 aluminium; *Acta Materialia*; Vol. 51; pp. 713–729
- [8] Li Y., Murr L.E. and McClure J.C.; (1999) ; Flow visualization and residual microstructures associated with the friction-stir welding of 2024 aluminum to 6061 aluminum; *Materials Science and Engineering*; Vol.; A271; pp.213–223
- [9] Krishnan K.N.; (2002); On the formation of onion rings in friction stir welds; *Materials Science and Engineering*, Vol. A327; pp. 246–251
- [10] Kumar K. and Kailas S. V.; (2008); The role of friction stir welding tool on material flow and weld formation; *Materials Science and Engineering*, Vol. A 485; pp. 367–374
- [11] El-Rayesa M. M. and El-Danaf E. A.; (2012); The influence of multi-pass friction stir processing on the microstructural and mechanical properties of Aluminum Alloy 6082; *Journal of Materials Processing Technology*; Vol. 212; pp. 1157–1168
- [12] Santella M.L., Engstrom T., Storjohann D. and Pan T.Y.; (2005); “Effects of friction stir processing on mechanical properties of the cast aluminum alloys A319 and A356”; *Scripta Materialia*, Vol 53, pp 201–206.
- [13] Ma Z.Y., Sharma S.R. and Mishra R.S.; (2006); Effect of friction stir processing on the microstructure of cast A356 aluminum; *Materials Science and Engineering*; Vol. A 433; pp. 269–278
- [14] Hofmann D. C. and Vecchio K. S.; (2005); submerged friction stir processing (SFSP): An improved method for creating ultra-fine-grained bulk materials; *Materials Science and Engineering*; Vol. A 402; pp. 234–241
- [15] Ceschini L., Boromei I., Minak G., Morri A. and Tarterini F.; (2007); “ Effect of friction stir welding on microstructure, tensile and fatigue properties of the AA7005/10 vol.%Al₂O₃p composite” *Composites Science and Technology*; Vol. 67; pp. 605–615
- [16] Hwang Y. M., Kang Z. W., Chiou Y. C. and Hsu H. H.; (2008); Experimental study on temperature distributions within the workpiece during friction stir welding of aluminum alloys ;*International Journal of Machine Tools & Manufacture*; Vol. 48; pp. 778–787
- [17] Kemal M., Kulekci, Esme U. and Buldum B.; (2015); Critical analysis of friction stir-based manufacturing processes; *Int J Adv Manuf Technol*
- [18] Bahrami M., Dehghani K., Givi M.K.B.; (2013); “A novel approach to develop aluminium matrix nano-composite employing friction stir welding technique”; *Materials and Design*.
- [19] Commin L., Dumont M., Masse J.-E., and Barrallier L.; (2009); Friction stir welding of AZ31 magnesium alloy rolled sheets: Influence of processing parameters; *Acta Materialia*; Vol. 57; pp. 326–334
- [20] [20] Jata K.V. and Semiatin S.L.; (2000); continuous dynamic recrystallization during friction stir welding of high strength aluminum alloys; *Scripta mater.*; Vol. 43; pp 743–749
- [21] Bussu G. And Irving P.E.; (2003); the role of residual stress and heat affected zone properties on fatigue crack propagation in friction stir welded 2024-T351 aluminium joints, *International Journal of Fatigue* Vol. 25 ; pp. 77–88
- [22] Ouyang J., Yarrapareddy E. and Kovacevic R.; (2006); Microstructural evolution in the friction stir welded 6061 aluminum alloy (T6-temper condition) to copper; *Journal of Materials Processing Technology*; Vol. 172; pp. 110–122
- [23] Rhodes C.G., Mahoney M.W., Bingel W.H. and Calabrese M.; (2003); Fine-grain evolution in friction-stir processed 7050 aluminum; *Scripta Materialia*; Vol. 48; pp. 1451–1455
- [24] Elangovan K. and Balasubramanian V.; (2008b); Influences of tool pin profile and welding speed on the formation of friction stir processing zone in AA2219 aluminium alloy; *Journal of materials processing technology* ; Vol. 2 00 ; pp. 163 – 175.
- [25] Moreira P.M.G.P., Santos T., Tavares S.M.O., Richter-Trummer V., Vilaça P., and de Castro P.M.S.T.; (2009); Mechanical and metallurgical characterization of friction stir welding joints of AA6061-T6 with AA6082-T6; *Materials and Design*; Vol 30; pp 180–187
- [26] Peel M., Steuwer A., Preuss M., and Withers P.J.; (2003); Microstructure, mechanical properties and residual stresses as a function of welding speed in aluminium AA5083 friction stir welds; *Acta Materialia*, Vol. 51; pp. 4791–4801
- [27] Liu G., Murr L.E., Niou C-S., McClure J.C., and F.R. Vega; (1997); Microstructural aspects of the friction-stir welding of 6061-T₆ aluminum; *Scripta Materialia*; Vol. 37, pp. 355-361
- [28] Su J. -Q, Nelson T. W., and Sterling C. J.; (2005); Microstructure evolution during FSW/FSP of high strength aluminum alloys; *Materials Science and Engineering*; Vol. A 405; pp. 277–286
- [29] Rhodes C.G., Mahoney M.W., Bingel W.H., Spurling R.A. and Bampton C.C.; (1997); Effects of friction stir welding on microstructure of 7075 aluminum; *Scripta Materialia*; Vol. 36; pp. 69-15.
- [30] Cam G. and Mistikoglu S.; (2014) Recent Developments in Friction Stir Welding of Al-alloys; *Journal of Materials Engineering and Performance*